Neuron, Vol. 47, 395–406, August 4, 2005, Copyright ©2005 by Elsevier Inc. DOI 10.1016/j.neuron.2005.06.019

The S4 Voltage Sensor Packs Against the Pore Domain in the KAT1 Voltage-Gated Potassium Channel

Helen C. Lai,[1,2] Michael Grabe,[2] Yuh Nung Jan,[2] and Lily Yeh Jan[2,*]
[1]Graduate Group in Biophysics
University of California, San Francisco
San Francisco, California 94143
[2]Departments of Physiology and Biochemistry
Howard Hughes Medical Institute
University of California, San Francisco
San Francisco, California 94143

Summary

In voltage-gated ion channels, the S4 transmembrane segment responds to changes in membrane potential and controls channel opening. The local environment of S4 is still unknown, even regarding the basic question as to whether S4 is close to the pore domain. Relying on the ability of functional KAT1 channels to rescue potassium (K^+) transport-deficient yeast, we have performed an unbiased mutagenesis screen aimed at determining whether S4 packs against S5 of the pore domain. Starting with semilethal mutations of surface-exposed S5 residues of the KAT1 pore domain, we have screened randomly mutagenized libraries of S4 or S1–S3 for second-site suppressors. Our study identifies two S4 residues that interact in a highly specific manner with two S5 residues in the middle of the membrane-spanning regions, supporting a model in which the S4 voltage sensor packs against the pore domain in the hyperpolarized, or "down," state of S4.

Introduction

Voltage-gated potassium (K_v) channels are widely distributed and perform numerous physiological functions in the animal and plant kingdoms. Plant K_v channels play important roles in controlling the flow of salt and water (potassium uptake and translocation toward the shoots) and in regulating cell volume (stomatal movement and root hair growth) (Brownlee, 2002; Gaymard et al., 1998; Hosy et al., 2003; Rodriguez-Navarro, 2000; Very and Sentenac, 2003), whereas animal K_v channels control the excitability of neurons and muscles and have been linked to diseases of the brain (epilepsy and episodic ataxia), ear (deafness), muscle (myokymia), and heart (arrhythmia) (Ashcroft, 2000; Crunelli and Leresche, 2002; Hille, 2001; Shieh et al., 2000). The basic mechanism for voltage gating—the ability of K_v channels to detect changes in membrane potential and respond with conformational changes that lead to channel opening or closing—is conserved in plant and animal K_v channels, though still not well understood at the molecular level.

There is a high degree of structural similarity between animal and plant K_v channels (Cao et al., 1995; Sato et al., 2002, 2003; Schroeder et al., 1994; Uozumi et al., 1998). Both are composed of four α subunits, each containing six transmembrane (6-TM) segments labeled S1 through S6. The pore-forming region, S5–S6, makes up the ion conduction pathway, and both channel types contain the potassium-selective signature sequence GYG. Both Shaker and KAT1, representatives from each family, require salt bridge interactions between conserved residues in S2 and S4 in order to fold and function (Sato et al., 2003; Seoh et al., 1996; Tiwari-Woodruff et al., 1997), and the S3–S4 linkers of each are exposed to the extracellular side (Gandhi et al., 2003; Lee et al., 2003; Mura et al., 2004). Moreover, chimeric constructs of KAT1 and *Xenopus laevis* Shaker form functional channels (Cao et al., 1995). Most importantly, the S4 segments of both plant and animal K_v channels contain multiple positively charged residues. Biophysical studies of voltage-gated sodium and potassium channels have shown that these channels contain intrinsic voltage sensors, S1–S4 (Bezanilla, 2000; Hille, 2001; Hoshi, 1995; Swartz, 2004; Yellen, 2002). In particular, the highly charged S4 segment is the primary component of the voltage sensor (Aggarwal and MacKinnon, 1996; Latorre et al., 2003b; Marten and Hoshi, 1998; Seoh et al., 1996; Sigworth, 1994; Zei and Aldrich, 1998).

In voltage-gated ion channels, the S4 basic residues are closer to the cytoplasmic side of the membrane (the "down" state) during hyperpolarization but move toward the extracellular side of the membrane (the "up" state) upon depolarization. Membrane depolarization drives S4 from the down state to the up state, causing depolarization-activated K_v channels to open (Bezanilla, 2002; Gandhi and Isacoff, 2002; Horn, 2002). In contrast, hyperpolarization-activated cation channels activate when S4 moves from the up state to the down state (Latorre et al., 2003b; Mannikko et al., 2002; Sesti et al., 2003). These differences in activation are likely due to different ways of coupling the voltage sensor to pore opening. Both depolarization- and hyperpolarization-activated channels have been found in kingdoms and domains ranging from archea to animals. For example, KvAP, SKOR, and Shaker are depolarization-activated channels from archea, plant, and animal, respectively (Gaymard et al., 1998; Ruta et al., 2003; Tempel et al., 1987). Hyperpolarization-activated channels of these same classifications are MVP, KAT1, and HCN (Anderson et al., 1992; Ludwig et al., 1999; Sesti et al., 2003). The high degree of gating and structural similarities of voltage-gated channels suggests that studying plant K_v channels will elucidate basic themes common to all K_v channels, including animal K_v channels found in neurons, heart, and muscle cells.

Crucial to the mechanistic understanding of voltage gating is the question of the location and surroundings of the S4 segment in the down state and the up state as well as along the gating transition pathway (Grabe et al., 2004). However, the existing models are rather divergent. Whereas several models suggest that S4 resides within the transmembrane domain in the down

*Correspondence: gkw@itsa.ucsf.edu

state and is at least partially surrounded by S1–S3 and S5–S6 (Broomand et al., 2003; Gandhi et al., 2003; Laine et al., 2003; Lee et al., 2003; Starace and Bezanilla, 2004), a different model, based upon the X-ray crystallographic data of the bacterial K_v channel, KvAP, bound to a Fab fragment (Jiang et al., 2003a), has S3b and S4 forming a paddle exposed at the periphery of the channel—far from S5, with S2 between the paddle and the pore domain—in the down state (Jiang et al., 2003a, 2003b). As to the up state of KvAP, electron microscopic analysis suggests that S4 is positioned loosely at the channel periphery with its basic residues exposed to the membrane (Jiang et al., 2004; Sands et al., 2005). Another up state model of KvAP based on electron paramagnetic resonance (EPR) spectroscopy has S4 on the periphery of the channel with most of the basic residues not exposed to the lipid (Cuello et al., 2004).

There has been much effort devoted to experimentally resolving the location of the S4 segment relative to the pore domain in K_v channels. Studies of the mammalian HERG and HCN2 channels, as well as chimeras between the 6-TM Shaker channel and the 2-TM KcsA channel, suggest close proximity of the cytoplasmic S4–S5 linker and the cytoplasmic end of S6 in the down state (Decher et al., 2004; Lu et al., 2002; Tristani-Firouzi et al., 2002). Moreover, cysteines introduced at the extracellular ends of S4 and S5 of the Shaker K_v channel can form disulfide bonds revealing close proximity between the ends of these segments in both the up and down states (Broomand et al., 2003; Gandhi et al., 2003; Laine et al., 2003; Neale et al., 2003). Attempts to induce disulfide bridge formation between cysteines within the S4 and S5 transmembrane segments have been unsuccessful (Gandhi et al., 2003; Laine et al., 2003); however, cysteines may not be as reactive in the hydrophobic environment of the protein/membrane core (Mordoch et al., 1999). Thus, whether S4 packs against S5 along their transmembrane segments remains an open question.

To circumvent these difficulties, we employed an alternative strategy involving random mutagenesis and a positive growth selection based on the ability of functional plant K_v channels to rescue the growth of the K^+ transport-deficient (*Δtrk1Δtrk2*) yeast strain SGY1528 in low-K^+ media (Anderson et al., 1992; Ko and Gaber, 1991). To date, it has not been possible to rescue K^+ transport-deficient yeast with mutant or wild-type animal K_v channels. Therefore, it is necessary to use hyperpolarization-activated plant K_v channels that are uniquely suited for this system due to their ability to selectively pass K^+ ions at the hyperpolarized membrane potential of yeast, estimated to be between –100 and –250 mV (Latorre et al., 2003a; Serrano and Rodriguez-Navarro, 2001). We have selected KAT1, a hyperpolarization-activated voltage-gated K^+ channel from *Arabidopsis thaliana* (Anderson et al., 1992; Schachtman et al., 1992), to carry out this study.

In this study, semilethal mutations are first introduced into the middle of the S5 segment so that the mutant KAT1 channel can rescue K^+ transport-deficient yeast for growth in 2 mM (selective) but not 0.4 mM K^+ (highly selective) media. If S4 packs against S5 within the transmembrane domain, a reduction of the channel function due to the semilethal mutation in the middle of S5 could conceivably be rescued by a second-site suppressor mutation in the middle of S4—such functional double mutant channels could in principle be selected from a library of KAT1 channels bearing the semilethal S5 mutation and a randomly mutagenized S4 segment. Likewise, similar screens of libraries of KAT1 channels bearing the same semilethal S5 mutation and randomly mutagenized S1–S3 segments would provide an opportunity of finding experimental support of S5 packing against the S1–S3 transmembrane segments. By constructing both types of libraries for mutant screens using yeast growth as a positive selection, we wished to search for evidence of specific interactions between the voltage-sensing domain and S5 residues within the transmembrane domain of K_v channels.

Results

The 6-TM K_v channels contain two functionally distinct transmembrane domains: the voltage sensor domain of S1–S4 and the pore domain of S5–S6 (Figure 1A). Because the outer helix of the pore domain, S5, is positioned to interact with the voltage sensor domain, our attempt to identify transmembrane segments that pack against the pore domain began with a search for mutations in the S5 segment that rendered the mutant KAT1 channel incapable of rescuing the K^+ transport-deficient (*Δtrk1Δtrk2*) yeast strain SGY1528 for growth on 0.2 or 0.4 mM K^+ (highly selective, low-K^+) media. These semilethal mutant channels were folded and expressed on the cell membrane, because they supported yeast growth on 2 mM K^+ (selective, see below) media. We then screened libraries of KAT1 channels carrying a semilethal S5 mutation and a randomized region of the voltage-sensing domain, either S1–S3 or S4, for functional rescue of the SGY1528 yeast strain. KAT1 channels carrying multiple mutations were isolated based on their ability to support yeast growth. In cases where specific suppressors emerged repeatedly from the screens, the specific mutation needed to suppress the original S5 semilethal mutation was identified and verified by constructing double mutants of the suppressor mutation together with the S5 semilethal mutation and showing that the suppressor complemented the S5 semilethal mutation not only in functional rescue of K^+ transport-deficient yeast, but also in functional expression of K^+ channels in *Xenopus* oocytes, as described below.

Identification of Semilethal Mutations in S5

A BLAST search was performed to the *Arabidopsis* KAT1 sequence (gi: 15237407) revealing 30 highly homologous, distinct channels, with a BLAST index of 500 and greater. A multiple alignment using ClustalW revealed five strictly conserved amino acids in S5 with a roughly helical periodicity (Thompson et al., 1994). All five S5 residues are on the surface of a structural model constructed of the KAT1 pore domain based upon the bacterial K_v channel KvAP using the program Modeller6v2 (Jiang et al., 2003a; Sali and Blundell, 1993); they project away from the central axis of the pore (Figure 1B). This finding agrees with the identification of outward-facing high-impact residues based on tryptophan scanning of the Shaker S5 segment (Li-Smerin et

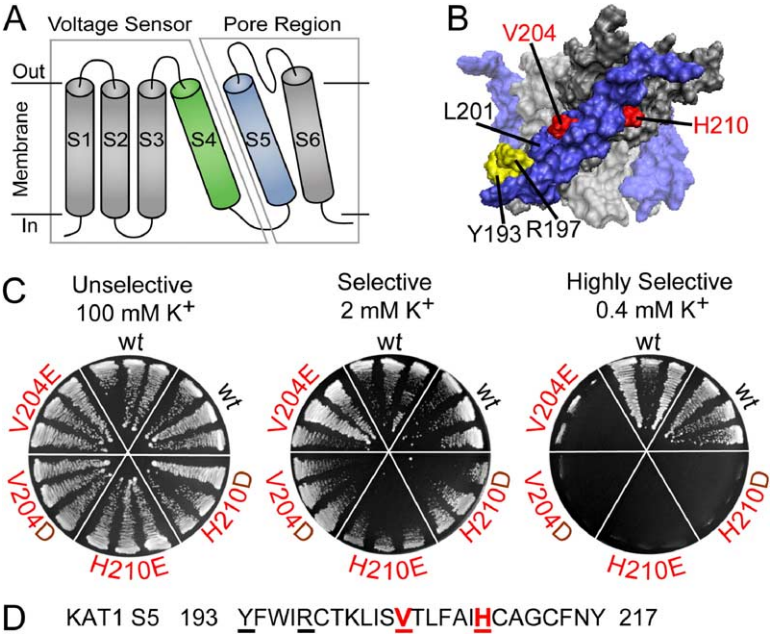

Figure 1. Identification of KAT1 Semilethal Mutations in S5

Glu (E) semilethal mutations are in red. Asp (D) semilethal mutations are in brown. (A) General topology of a 6-TM subunit of the tetrameric K_v channel, with the voltage sensor S1–S4 and the pore region S5–S6 outlined. Transmembrane segments are shown as rods and loop regions as curved lines. The extracellular region is designated as "out" and the intracellular region is designated as "in." (B) The S5 residues Y193 (yellow), R197 (yellow), L201, V204 (red), and H210 (red) highlighted on a model of the KAT1 pore domain, S5–S6, reveal that all 5 residues are on the surface of the pore domain, with V204 and H210 well within the predicted transmembrane segment of S5. S5 is shown in blue and S6 in gray, the subunit closest to the reader in darker shade than the remaining 3 subunits. Loop regions were not included in the figure for clarity. (C) All constructs, wt, V204E, V204D, H210E, and H210D grow on unselective 100 mM K^+ media and also on the selective 2 mM K^+ media. However, V204E, V204D, H210E, and H210D cannot rescue the K^+ transporter-deficient yeast on the highly selective 0.4 mM K^+ media. (D) The KAT1 S5 sequence including V204 and H210 (red and underlined) and Y193 and R197 (black and underlined), based on a published alignment (Shealy et al., 2003).

al., 2000) and suggests that S5 of the pore domain is in contact with another part of the channel.

We mutated these strictly conserved residues in S5 to glutamate (E), aspartate (D), or glutamine (Q) and tested whether these mutant channels could support yeast growth on low-K^+ media. Glutamate substitution of four of these S5 residues (highlighted in Figure 1B), Y193, R197, V204, and H210, as well as glutamine substitution of R197, and aspartate substitution of V204 or H210, prevented the mutant channel from rescuing yeast growth on 0.4 mM K^+ (highly selective) media, whereas these mutant channels were compatible with yeast growth in media containing 100 mM (unselective) or 2 mM K^+ (selective) (Figure 1C and data not shown). The ability of these semilethal S5 mutants to support yeast growth in 2 mM K^+ media indicates that the mutant KAT1 channels are folded and functional to some extent, since negative controls of KAT1 with insertion of unrelated protein (KAT1-S1-S3-stuffer and KAT1-S4-stuffer fusion proteins—see Experimental Procedures) do not support growth on 2 mM K^+ media (data not shown). The strong detrimental effect of the semilethal mutation is likely due to compromised interactions of the S5 segment with the rest of the channel protein surrounding the pore domain, since our model of the KAT1 pore domain predicts that these S5 residues are exposed on the surface of the pore domain (Figure 1B, red and yellow). In particular, V204 and H210 are located well within the vertical extent of the membrane (Figure 1B, red), far from either end of the S5 segment, with at least seven flanking residues (Figure 1D) (Shealy et al., 2003).

Screening for Interactions between S5 and S1–S4

To test whether the voltage sensor packs against S5, we screened libraries of KAT1 channels carrying one of the following S5 semilethal mutations, Y193E, R197E or Q, V204E or H210E, along with randomly mutagenized S1–S3 segments or a randomly mutagenized S4 segment. Thus, each set of experiments involved one S5 semilethal mutation screened against a library of S1–S3 or S4. Channels that acquired compensatory mutations in S1–S3 or S4, thereby suppressing the semilethal S5 mutations and permitting yeast growth, were isolated (see Table 1, parts A and B, for screening data). Interestingly, the outcome of the screens fell into two distinct categories: constructs with highly specific mutations—recovered repeatedly—that supported more robust yeast growth (class I) and constructs with more diverse mutations that were recovered at much lower frequencies, likely due to weaker yeast growth (class II).

Screening several thousand constructs with mutagenized S1–S3 and a specific S5 semilethal mutation resulted in less than 0.5% rescued colonies on low-K^+ media from each individual screen (Table 1, part A) with no clear pattern of second-site suppressor mutations (class II). Despite different overall patterns, many constructs shared common mutations in S1–S3 irrespective of the initial S5 semilethal mutation (see Figure S1 in the Supplemental Data available online). Therefore, some of these S1–S3 mutations have enhanced channel activity in a manner that is not specific to the S5 semilethal mutations that they suppressed.

Both classes of suppressor mutations were obtained from the S4 mutant library screens. For the S5 semilethals, Y193E and R197Q, the outcome was similar to what we observed with the S1–S3 mutant library screens, with less than 0.15% rescued colonies on low-K^+ media (class II) (Table 1, part B). By contrast, a unique S4 suppressor was repeatedly isolated from all of the sampled colonies recovered on highly selective media in the S4 library screens against either V204E or H210E S5 semilethals (Table 1, part B) with greater than 1.1% rescued colonies on low-K^+ media (class I). The double mutants

Table 1. Summary of Yeast Screens of Mutant Libraries

A S5 semilethals screened against an S1-S3 library.

Semilethal Mutation	Library Complexity	# Screened	Estimated % Rescue	Specific Suppressor
Y193E	5.9×10^5	3144	0.25	N/A
R197E	6.0×10^4	8500	0.31	N/A
V204E	5.8×10^4	5796	0.50	N/A
H210E	1.2×10^5	6757	0.18	N/A

B S5 semilethals screened against an S4 library.

Semilethal Mutation	Library Complexity	# Screened	Estimated % Rescue	Specific Suppressor
Y193E	4.4×10^4	3083	0.13	N/A
R197Q	1.7×10^4	7748	0.15	N/A
V204E	1.0×10^4	8988	2.1	**S179N**
H210E	2.1×10^4	6840	1.1	**M169L**

C S5 semilethals screened against a randomized codon of the putative second-site suppressor.

Semilethal Mutation	Library Complexity	# Screened	Estimated % Rescue	Recovered Mutation
V204E	272	1040	5.7	**S179N**
V204D	2904	2361	0	None
H210E	288	958	14	**M169L**
H210D	609	2113	6.4	**M169L**

N/A means not applicable. (A) Data for screening libraries containing an S5 semilethal and a randomly mutagenized S1–S3. The suppressors recovered for each S5 semilethal, Y193E, R197E, V204E, and H210E, have multiple mutations, but do not share a single mutation specific for the S5 semilethal. The estimated percent rescue is less than 0.5% for all these screens. (B) Data for screening libraries containing an S5 semilethal and a randomly mutagenized S4. For screens against the Y193E and R197Q semilethals, no specific suppressor emerged and the estimated percent rescue is less than 0.15%. By contrast, S4 library screens against the S5 semilethals, V204E and H210E, were rescued in greater than 1.1% of the colonies. They were suppressed by highly specific S4 mutations; the same suppressor was found in each colony growing on low-K^+ media that was analyzed. Thus, S179N and M169L (purple) specifically suppressed V204E and H210E (red), respectively. (C) Data for screening libraries containing an S5 semilethal (red or brown) mutation and randomized codon of the S4 residue yielding the second-site suppressor (purple).

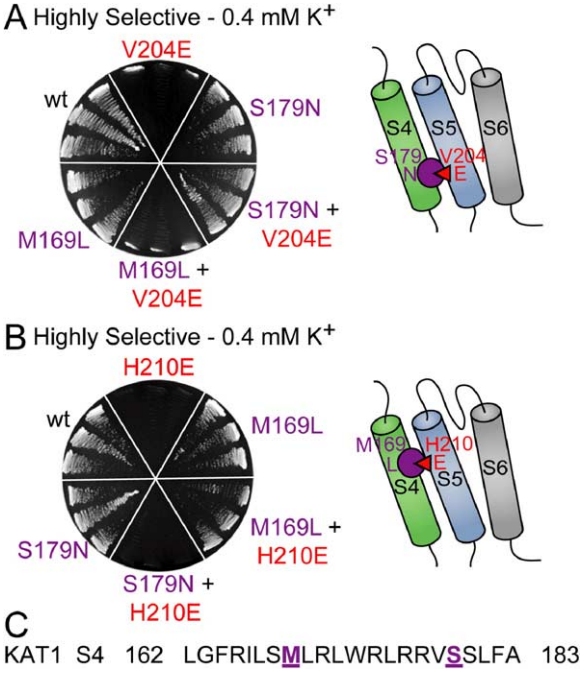

Figure 2. S4 Second-Site Suppressors Are Specific for S5 Semilethal Mutations

(A) S179N (but not M169L) suppression of the detrimental effect of the V204E mutation, shown schematically on the right, allows the double mutant to support yeast growth on 0.4 mM K^+. (B) Double mutant rescue of yeast growth on 0.4 mM K^+ due to M169L (but not S179N) suppression of the detrimental effect of H210E, shown schematically on the right. (C) The KAT1 S4 sequence including M169 and S179 (purple and underlined) with boundaries as reported (Anderson et al., 1992).

S179N+V204E and M169L+H210E rescued K^+ transport-deficient yeast (Figures 2A and 2B). Unlike the single S5 mutants V204E and H210E, the S179N and M169L single mutations did not impair the ability of KAT1 channels to rescue mutant yeast (Figures 2A and 2B), probably due to the more conservative nature of these S4 mutations. The suppression of the S5 semilethal mutations by these S4 mutations, well within the transmembrane segment (Figure 2C), is specific, since the double mutants S179N+H210E and M169L+V204E failed to support yeast growth (Figures 2A and 2B).

The S4 mutations suppressed the S5 semilethals without increasing channel protein expression. HA-tagged double mutants containing the S4 suppressor and the S5 semilethal had comparable or less expression than the HA-tagged S5 semilethal alone (Figure S2). Moreover, epifluorescence microscopy revealed comparable levels of surface expression in yeast expressing EGFP-tagged S5 semilethal mutant channels or double mutant channels carrying the S5 mutation together with its S4 suppressor (Figure S3). All KAT1 constructs tagged with either HA or EGFP gave the same yeast growth phenotypes as the untagged versions. Taken together with the fact that the S5 semilethal mutant must have yielded functional channels on the cell membrane to rescue yeast grown on 2 mM K^+, these observations support the notion that the suppression takes place in functional channels on the cell membrane.

Functional Expression of the Double Mutants in *Xenopus* Oocytes

The double mutant of the S5 semilethal mutation together with its specific S4 suppressor yielded greater currents in *Xenopus* oocytes than the single S5 mutant did, as expected from the greater capacity of the double mutant to rescue yeast growth. Having eliminated the endogenous hyperpolarization-activated chloride currents and cation currents (Kuruma et al., 2000) by using chloride-free solutions for recording and by adding 1 mM Ba^{2+} as a channel blocker (Figure 3A), we found no detectable currents in oocytes expressing the H210E semilethal mutant that failed to rescue yeast grown on 0.5 mM or lower K^+ media, whereas the single S5 mutant V204E—which supported yeast growth on 0.5 mM, but not 0.4 mM K^+ media—generated very low levels of currents compared to wild-type KAT1 (Figures 3B and 3C). Inclusion of the specific S4 suppressor in the double mutant led to greater currents than those due

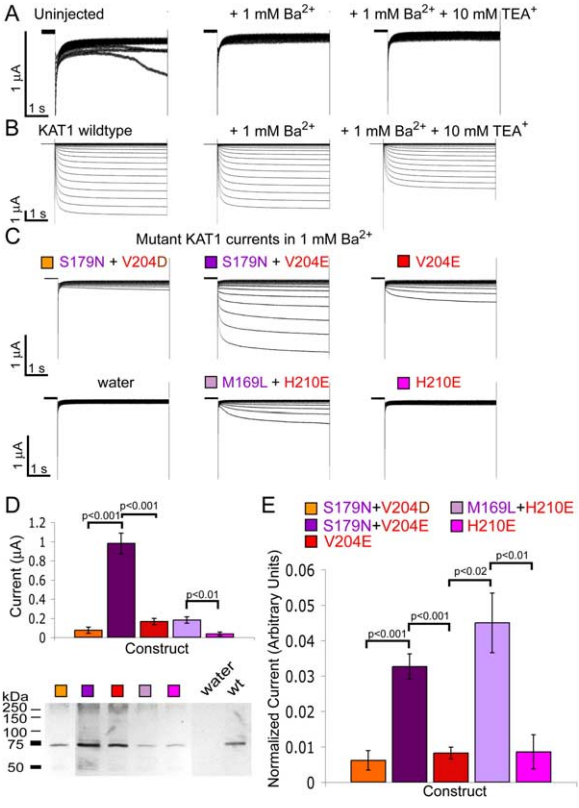

Figure 3. Mutant KAT1 Currents and Protein Expression

Oocytes expressing KAT1 wild-type were subjected to voltage pulses from +20 mV to –180 mV in 10 mV increments for a duration of 5 s each, from a holding potential of –10 mV, whereas hyperpolarizations from –70 mV to –180 mV were given to uninjected and water-injected oocytes and those expressing the semilethals and double mutants. KAT1 constructs containing a C-terminal HA tag were used in oocyte expression for both current recordings and protein expression measurements. (A) Endogenous hyperpolarization-activated currents, apparent at potentials more negative than –160 mV in uninjected oocytes (left), is blocked by 1 mM Ba^{2+} (middle) and undetectable after addition of 1 mM Ba^{2+} and 10 mM TEA^{+} (right). (B) Current due to KAT1 wild-type channels (left) is slightly reduced by 1 mM Ba^{2+} (middle) and is further blocked by 10 mM TEA^{+} (right). Oocytes were recorded 4 days after 5 ng cRNA injection. (C) The S179N+V204E double mutant gives more current compared to the V204E semilethal and the S179N+V204D double mutant, both of which cannot rescue yeast growth on 0.4 mM K^{+}. Likewise, the M169L+H210E double mutant gives more current than the H210E mutant. All traces are from the same batch of oocytes, except for S179N+V204D. (D) (Top) Steady-state current amplitudes of KAT1 double mutants and semilethals at –160 mV in barium-blocking solution after subtraction of endogenous currents as measured in water-injected oocytes in barium-blocking solution (n = 5 for each construct, mean and standard errors shown). Constructs are color coded as indicated in (E). (Bottom) Western blot of KAT1 constructs from oocytes. All the double mutants and semilethals are for oocytes injected with 30 ng RNA and after 5.5–6 days expression. Oocytes from the 50 nL water-injected control were taken 6 days after water injection, while the 30 ng injected KAT1-HA wild-type control was taken after 3 days. All bands are from the same gel with the same exposure time in the linear range of the film. Lanes were rearranged to align with the graphs. (E) Single and double mutant KAT1 currents were normalized by the total channel protein expression in oocytes as determined from the Western blot in (D) from the average pixel intensity of each band with background subtraction.

to the respective S5 semilethal single mutants (Figure 3C) (S179N+V204E, V204E, $p < 0.001$; M169L+H210E, H210E, $p < 0.01$; Figure 3D). When the current amplitudes were normalized for total channel protein (Figure 3D), four pairwise comparisons revealed that the mutants that rescued yeast growth on 0.4 mM K^{+} yielded more current than those that did not (S179N+V204E, V204E, $p < 0.001$; M169L+H210E, H210E, $p < 0.01$; M169L+H210E, V204E, $p < 0.02$; S179N+V204E, S179N+V204D, $p < 0.001$; Figure 3E).

The mutant channels displayed pharmacological properties characteristic of KAT1 channels, but required greater hyperpolarization for their activation. KAT1 was slightly reduced by 1 mM Ba^{2+} and further reduced by 10 mM TEA^{+} (tetraethylammonium) (Schachtman et al., 1992) (Figure 3B), while the endogenous hyperpolarization-activated currents were blocked only by 1 mM Ba^{2+} (data not shown). Like wild-type KAT1 channels, the single mutants and double mutants were TEA^{+} sensitive (data not shown). Whereas the double mutants activated at more hyperpolarized potentials than wild-type KAT1 channels (note that all current traces in Figure 3C were induced by greater hyperpolarization pulses), their voltage dependence appeared to be in between that of the S5 semilethal single mutants and the wild-type channel, because the S5 single mutants yielded smaller or nondetectable currents even at the most hyperpolarized membrane potential tested. Thus, while the oocyte recordings may not have revealed the magnitude of the mutant channel activity at the yeast membrane potential, these electrophysiological experiments support the notion that the specific interaction between the S5 semilethal mutations and their respective S4 suppressors increased the ability of channels containing an S5 semilethal mutation to conduct K^{+} currents at the yeast's hyperpolarized membrane potential, thereby allowing the double mutants to support yeast growth not only at 2 mM K^{+} (selective), but also at 0.4 mM K^{+} (highly selective).

For the rest of the study, we have focused on the specificity of the interaction between S179N and V204E and between M169L and H210E. These specific second-site suppressors of the semilethal S5 mutations, V204E and H210E, are located roughly in the middle of the S4 segment (Figure 2C), at least four residues from either end (Anderson et al., 1992), far from both the cytoplasmic S4–S5 loop and residues at the extracellular end of S4 that are in close proximity to the extracellular end of S5 (Broomand et al., 2003; Decher et al., 2004; Gandhi et al., 2003; Laine et al., 2003; Lu et al., 2002; Mannikko et al., 2002; Neale et al., 2003; Tristani-Firouzi et al., 2002). The locations of these specific S4 mutations are compatible with the expectation that the second-site suppressors are adjacent to the semilethal mutations of the S5 segment, lending support to the notion that S4 packs against S5 within the membrane-spanning region.

Effects of Shortening the S5 Side Chain Length on the Suppression of Channel Semilethality by the S4 Mutation

We began our analysis of the specificity of suppression by first asking whether the same S4 mutation could suppress the semilethal mutation due to substitution

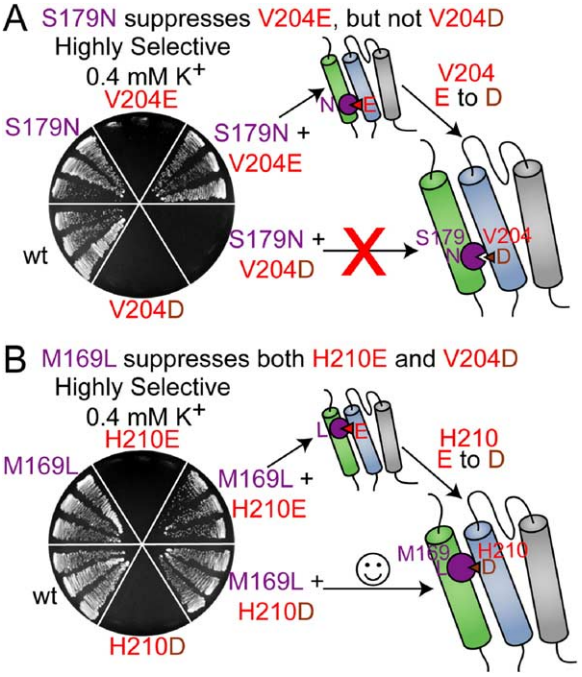

Figure 4. Test of the Sensitivity of Second-Site Suppression on the Semilethal Mutation Side Chain Length

One of the S4 suppressors (purple) for S5 glutamate (E) substitution (red) cannot suppress the aspartate (D) substitution of the same S5 residue (small brown triangles). (A) S179N cannot suppress the V204D semilethal on 0.4 mM K^+. (B) M169L can suppress the H210D semilethal on 0.4 mM K^+.

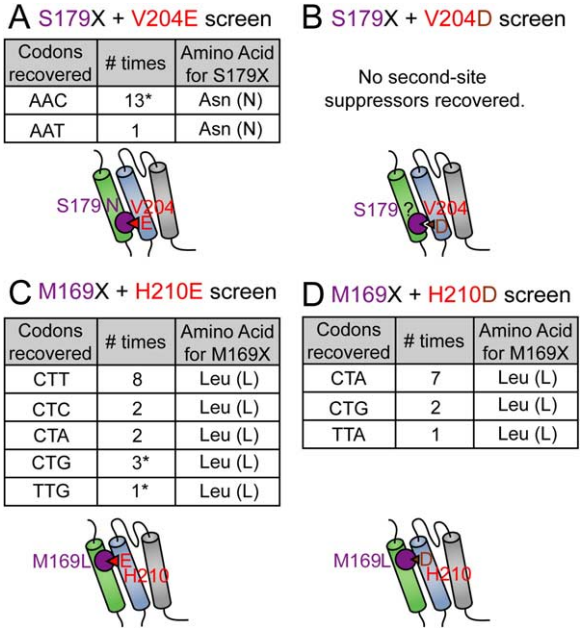

Codons recovered	# times	Amino Acid for S179X
AAC	13*	Asn (N)
AAT	1	Asn (N)

Codons recovered	# times	Amino Acid for M169X
CTT	8	Leu (L)
CTC	2	Leu (L)
CTA	2	Leu (L)
CTG	3*	Leu (L)
TTG	1*	Leu (L)

Codons recovered	# times	Amino Acid for M169X
CTA	7	Leu (L)
CTG	2	Leu (L)
TTA	1	Leu (L)

Figure 5. Second-Site Suppressors Are Highly Specific for the S5 Semilethal

The tables indicate the codons (left column) encoding the amino acid (right column) recovered from the suppressor screens. Those codons detected in the original S4 library screen against that particular S5 semilethal (Figure 2 and Table 1) are marked by an asterisk (*) and included in the number of times that codon was detected (middle column). (A) S179X+V204E screen recovered only codons for Asn (N), the original second-site suppressor. (B) S179X+V204D screen recovered no suppressors. (C) M169X+H210E screen recovered only codons for Leu (L). (D) M169X+H210D screen also recovered only codons for Leu (L).

of the S5 residue with aspartate rather than glutamate. Interestingly, the S179N mutation of S4 could not suppress the semilethality of V204D (Figure 4A) when comparably expressed (Figure S2). Thus, the interaction between the polar asparagine substituting S179 on S4 and the glutamate semilethal mutation of V204 on S5 is highly sensitive to the side chain length.

In an analogous test, we found that the same S4 mutation, M169L, suppressed both H210E and H210D mutations, so that the double mutants, but not the single S5 mutants, supported yeast growth on 0.4 mM K^+ media (Figure 4B) when comparably expressed (Figure S2). The ability of the leucine substitution for the S4 methionine to enhance the function of mutant KAT1 channels with either glutamate or the smaller aspartate replacing the S5 histidine is likely due to hydrophobic interactions involving these side chains within the protein, since structural studies have shown that cavities created by shortening a side chain may be partially compensated for by small movements of surrounding atoms (Eriksson et al., 1992).

The S4–S5 Interactions Are Specific

To further scrutinize the specificity of the interaction between the S5 semilethal mutations and their respective S4 suppressors, we randomized the codon for the S4 residue at position 179 or 169 in channels carrying either aspartate or glutamate at the semilethal positions in S5, position 204 and 210, respectively (Figure 5). The randomized codon was created using a DNA primer containing NNN as the codon for the particular S4 residue, by mixing equal amounts of the four nucleotides at each of the three positions during primer synthesis. We then sequenced a number of mutant constructs from the library without subjecting them first to selection based on yeast growth to verify that all four nucleotides were represented at each of the three positions of that S4 codon.

After this extensive screen of libraries with a randomized S4 codon at position 179, we came to the surprising conclusion that only S179N can suppress the V204E semilethal S5 mutation. From a total of 13 colonies recovered on highly selective media, both asparagine codons were represented, but no codons for any other amino acids emerged from the mutant screen (Figure 5A). Moreover, a similarly exhaustive screen of libraries of KAT1 bearing the V204D rather than V204E semilethal S5 mutation gave rise to no viable yeast colonies on highly selective media (Figure 5B). We further used site-directed mutagenesis to generate the double mutant S179Q+V204D and verified that this double mutant could not rescue yeast on low-K^+ media (data not shown). Thus, evidently no amino acid at position 179 can accommodate the V204D mutation, further reinforcing the notion that the S179N suppression of V204E is highly specific.

The randomized screen of position 169 recovered only leucine as a viable suppressor of the H210D and H210E semilethal mutants. So, while M169L can rescue both H210D and H210E, the interaction between positions 169 and 210 is still highly specific. All possible codons for leucine were represented in ten suppressors of the S5 H210D mutant and 14 suppressors of the H210E mutant (Figures 5C and 5D), indicating that leucine at position 169 of the S4 segment is uniquely capable of packing against the S5 segment bearing the H210D or H210E mutation.

Discussion

To understand how the S4 segment of K_v channels could function as the voltage sensor by detecting changes in membrane potential and triggering conformational changes of the channel, it is important first to learn how the S4 segment is positioned relative to the rest of the channel protein. The use of yeast growth as a positive selection for the screening of randomly mutagenized K_v channels is crucial for identifying specific interactions between transmembrane segments in the absence of a structural guide, because thousands of mutants can be tested in an unbiased way to select for only folded and functional channels at the membrane surface. This approach has allowed us to uncover two highly specific interactions within the membrane-spanning regions of S4 and S5, likely occurring in the down state, since channel opening is required for yeast growth at 2 mM and lower K^+ concentrations (Figures 6A and 6B). The fact that mutation of the "lower" (closer to the cytoplasmic side) S4 residue suppressed the "lower" S5 semilethal and mutation of the "higher" (closer to the extracellular side) S4 residue suppressed the "higher" S5 semilethal is suggestive that these highly specific interactions reflect physical proximity between the S5 semilethals and their respective S4 suppressors.

Previous studies support the assertion that suppressors for semilethal mutations usually reside on neighboring structural elements. For example, a variation of the method used here was applied successfully using mutagenesis coupled with yeast screens to determine the transmembrane helix packing of the two-transmembrane K^+ channel Kir 2.1 (Minor et al., 1999), which turned out to be in excellent agreement with the crystal structure of a homologous channel, KirBac1.1 (Kuo et al., 2003). This case highlights that semilethal-second-site suppressor pairs lie on interacting surfaces of neighboring transmembrane helices or that these segments are packed closely enough to transmit suppression through other well-packed residues. It also provides a concrete example of how such yeast screens of randomly mutagenized channels can reveal accurate structural information.

Substitution of V204 of the S5 segment with either acidic residue aspartate or glutamate reduced KAT1 channel function to such an extent that the mutant channel could facilitate the growth of K^+ transport-deficient mutant yeast on 2 mM but not 0.4 mM K^+ media. The semilethal mutation V204E, but not V204D, was suppressed only by the S179N mutation in the S4 segment, suggesting a close interaction between these two residues. Similarly, both semilethal mutations H210D and H210E of the S5 segment were suppressed by exactly one mutation of the S4 segment, M169L. We have determined that these second-site suppressions are highly specific by carrying out multiple screens of different libraries of randomly mutagenized S4 residues; in no case were additional suppressors isolated (Table 1, part C; Figure 5). This complete specificity of the interactions between two residues in the middle of the S4 segment with two residues in the middle of the S5 segment is highly suggestive of close packing between the S4 and S5 segments. It is worth noting that other residues in the vicinity of the pair of S5 semilethal and S4 suppressor mutation likely participate in polar and

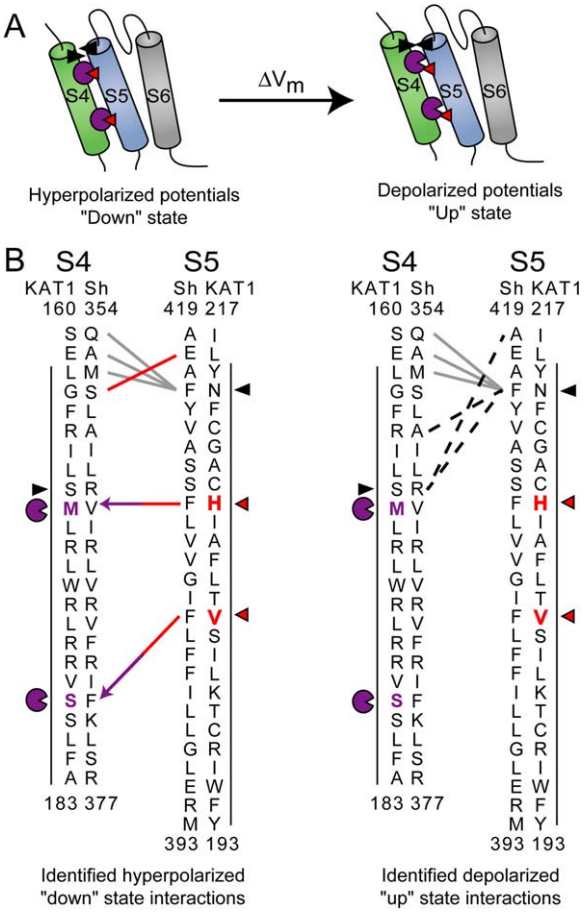

Figure 6. S4–S5 Interactions for KAT1 and Shaker K_v Channels

(A) Schematic summary of likely S4 motion relative to the pore domain. (B) Arrows link S5 semilethals (red triangles) to second-site suppressors found from the yeast screens (purple pacmans), interactions that enhance KAT1 channel activity in the hyperpolarized state (left). Based on published alignment of S4 (Latorre et al., 2003b) and S5 (Shealy et al., 2003), a down state disulfide bridge interaction for Shaker found by Neale et al. is designated by a red line (Gandhi et al., 2003; Neale et al., 2003), disulfide bridges found for the depolarized or up state of Shaker (right) are shown by dashed lines and marked with black triangles for R362C+F416C (Broomand et al., 2003; Gandhi et al., 2003; Laine et al., 2003), and disulfide bridges found in both the down and up states of Shaker by Gandhi et al. shown in gray (left and right) (Gandhi et al., 2003).

hydrophobic interactions, as a side chain within a protein typically interacts with parts of multiple side chains. Nonetheless, the highly specific interactions between S4 and S5 residues within these transmembrane segments lend strong support to the notion that the S4 voltage sensor packs against the pore domain.

Notably, the choice of semilethal S5 mutations that reduced, but did not abolish, KAT1 channel function in yeast (rescue of yeast growth at 2 mM and not 0.4 mM K^+) renders it highly unlikely that such mutations exert their impact by preventing folding of the channel. Whereas mutations that compromise protein folding could reduce protein levels, these S5 semilethal mutant channels gave similar levels of protein expression as those of the double mutants in *Xenopus* oocytes (Figure 3D) and in yeast (Figures S2 and S3). Not only did the combination of a semilethal S5 mutation with its specific S4 suppressor restore the ability to rescue yeast on 0.4 mM K^+ (Figure 2), the double mutant also yielded greater currents than the respective single S5 mutants in *Xenopus* oocytes (Figures 3C–3E). Inclusion of the S4 suppressor mutation may have caused some right shift of the voltage dependence curve compared to that of the S5 single mutants, though it was difficult to quantify these shifts when even the largest hyperpolarization tested was insufficient to allow the mutant channels to reach maximal activation. Taken together, the interactions between V204E and S179N and between H210E and M169L in the double mutants likely increase the channel activity in the open state, or down conformation, of the channel relative to that of the single S5 mutants, which rescue yeast growth on 2 mM but not 0.4 mM K^+, since a greater ability of K^+ conduction is necessary to support yeast growth in lower K^+ concentrations.

The class II mutations in S1–S3 or S4 provide evidence for close packing of the voltage sensor and the pore domain, for a different reason. Screens of S5 semilethals against an S1–S3 library revealed that this class of mutations was nonspecific in that no common mutation existed across all of the sampled constructs that suppressed a particular S5 semilethal and several mutations suppressed more than one S5 semilethal (see Figure S1). This is in contrast to the highly specific class I suppressors in S4, where each mutation uniquely compensates the detrimental effect of a particular S5 semilethal at position V204 or H210. Careful studies on globular proteins reinforce the notion that two regions of a protein in close apposition have stronger interactions than do two regions that are distant from each other (LiCata and Ackers, 1995; Schreiber and Fersht, 1995; Wells, 1990). This observation indicates that the class I suppressors are in close contact with the semilethal mutation, while class II mutations involve more distant allosteric interactions so that specific information about the chemistry of the substituted amino acid is lost as it is elastically transmitted through the protein to the initial semilethal site. It is also possible that class II mutations enhance the channel activity in a manner completely independent of the original S5 semilethal mutation, thus allowing channels bearing both the semilethal and the class II mutations to be more active.

Our findings of second-site suppressors in the S4 segment interacting in very specific ways with two S5 residues located within the vertical extent of the membrane provide strong evidence that the voltage sensor packs against the pore domain. In the only high-resolution structure of a K_v channel (Jiang et al., 2003a, 2003b), the S4 segment packs only against S3b and is separate from the pore domain. It is difficult to reconcile this structure, or the models based on this structure (Jiang et al., 2003a, 2003b), with our findings of second-site suppressors in the S4 segment interacting in very specific ways with two S5 residues located within the membrane. It is conceivable that the Fab fragments in the co-crystal trapped the channel in a rarely visited conformation (Cohen et al., 2003) or that the Fab fragments pulled the S4 segment down (Jiang et al., 2003a). Other confounding factors include the lack of a planar lipid membrane to support the correct juxtaposition of the pore domain and the voltage sensor domain and the possibility of these domains being incorporated into separate micelles (Gulbis and Doyle, 2004).

It is worth noting that the S4 residue M169 of KAT1 corresponds to the residue immediately following the first S4 basic residue of Shaker—R362 (Shealy et al., 2003). Furthermore, only when the Shaker channel is in the up state can the cysteine replacing R362 be cross-linked with a cysteine replacing either F416 or A419, at the extracellular end of S5 (Broomand et al., 2003; Gandhi et al., 2003; Laine et al., 2003) (Figure 6B). If the down state of KAT1 channel is indeed structurally analogous to the down state of Shaker channel, the highly specific interaction between M169 and a S5 residue within the confine of the membrane, two to three helical turns from the S5 residues corresponding to F416 and A419 of Shaker, would imply that the S4 segment moves outward—in the vicinity of the pore domain—as the channel transits from the down state to the up state (Figure 6A). This scenario for voltage gating of K_v channels is consistent with recent studies suggesting that S4 moves in a gating pore (Tombola et al., 2005), without concerted movement together with S3b as a paddle in the membrane (Ahern and Horn, 2004; Gonzalez et al., 2005).

The strategy of identifying specific second-site suppressors as reported in this study provides an unbiased paradigm to assess the proximity of transmembrane segments of K_v channels in a biological system. Using this approach, we have uncovered specific interactions over a large span of S4 and S5 suggesting that these two segments are in close proximity. Whether and how S1–S3 might pack against S4 is another question that could potentially be addressed in future studies employing yeast mutant screens. It is important to stress here the difference between S4 movement during voltage gating of K_v channels on the cell membrane and membrane insertion of S4 in the endoplasmic reticulum, a process that takes much longer and critically depends on the context—the hydrophobic segments that precede S4, the translocon, and probably chaperones as well (Hessa et al., 2005; Sato et al., 2002). The finding that the S4 helix has intimate contact with other portions of the channel within the membrane span has profound implications on the energetics of voltage gating (Grabe et al., 2004). Additionally, the close interactions between the voltage sensor S4 and the outer helix of the pore domain will be of critical importance in con-

sidering how the motion of the S4 sensor might influence the conformation of the pore domain in channel gating (Doyle, 2004; Swartz, 2004; Yellen, 2002).

Experimental Procedures

Molecular Biology

KAT1 with its 5′ and 3′ UTRs was amplified by PCR and cloned into the HindIII-XhoI sites of a modified pYES2 vector containing a Met-25 promoter (Minor et al., 1999). Site-directed mutations were made using the QuikChange site-directed mutagenesis kit (Stratagene, LaJolla,CA). For the yeast libraries, the following silent mutations were made: AvrII-SacI cut sites (at residues 57 and 161) flanking the DNA region coding for S1–S3 and SacI-BamHI cut sites (at residues 161 and 195) flanking the DNA region coding for S4. A stuffer sequence containing the N and C terminus (residues 1–96 and 192–414 linked with a GGSGG sequence in between) of Kir 3.2 was inserted between either the AvrII-SacI sites or the SacI-BamHI sites to create the KAT1-S1-S3-stuffer and KAT1-S4-stuffer constructs, providing negative controls and also a nonfunctional background for library construction. All constructs were verified by fluorescence sequencing.

Library Construction

Libraries were created using primers containing the AvrII-SacI cut sites flanking S1–S3 and the SacI-BamHI cut sites flanking S4 of KAT1 to amplify S1–S3 (residues 66–154) or S4 (168–189, or 168–184 for the Y193E screen) by error-prone PCR: 1× Taq Buffer, 0.2 mM dATP, 1 mM dGTP, 1 mM dCTP, 1 mM dTTP, 0.5 μM forward primer, 0.5 μM reverse primer, 100 ng double stranded DNA template, 4 mM $MgCl_2$, 0.5 mM $MnCl_2$, and 5 units of Taq polymerase (Promega, Madison, WI). This created a 2.1%–3% base pair error rate corresponding to 4.6%–5.3% amino acid changes per region in unselected clones.

Error-prone PCR products were gel purified and cut with the appropriate restriction enzymes and ligated into the KAT1-S1-S3-stuffer or KAT1-S4-stuffer constructs. Ligation mixtures were phenol/chloroform extracted, ethanol precipitated, and resuspended in 3 μl of autoclaved reagent grade water. 1 μl of the ligation mixture was used to transform DH10B competent cells (Invitrogen, Carlsbad, CA) via electroporation. The transformed cells were resuspended in 1 ml SOC and incubated at 37°C for 0.5–1 hr with shaking. 1 μl of these cells was plated onto LB + carbenicillin to determine library complexity, and the rest was added to 100 ml LB + carbenicillin liquid culture for growth overnight. The plasmids from the library culture were extracted using the Qiagen maxiprep kit (Qiagen, Valencia, CA) for use in the yeast-selection assay.

Randomized codons were created using the QuikChange site-directed mutagenesis kit (Stragene, LaJolla, CA) with primers containing NNN (25% A, C, G, T at each site) yielding 64 possible codons. A portion of the bacteria transformed with the QuikChange mixture was plated onto LB + carbenicillin plates, yielding colonies from which plasmids were extracted using the Qiagen miniprep kit (Qiagen, Valencia, CA) and sequenced by fluorescence sequencing to assess the mutation complexity. The number of colonies on the plate determines the library complexity. An equivalent portion was added to 100 ml LB + carbenicillin liquid culture for growth overnight. Plasmids from the library culture were extracted using the Qiagen maxiprep kit (Qiagen, Valencia, CA) for use in the yeast-selection assay. These libraries each contained more than 272 (500 in two cases) independent constructs (Table 1, part C) corresponding to a greater than 40% (97% in those two cases) confidence level that all possible codons (64) are represented.

Yeast Selection

The yeast strain SGY1528 was transformed with mutant libraries via lithium acetate and plated onto nonselective conditions containing 100 mM K^+ (Minor et al., 1999). After growth for 3 days, yeast were either replica plated successively onto plates containing 2 mM K^+, 0.5 mM K^+, and finally 0.2 mM K^+ or directly plated onto 0.4 mM K^+ media plates with 1–3 days of growth in between replica plating. Plasmids were extracted from the colonies that grew on 0.2 mM or 0.4 mM K^+ plates, used to retransform yeast to verify the phenotype, and sequenced to identify mutations. Growth phenotypes were assessed by plating yeast transformed with wild-type or mutant KAT1 on 100 mM K^+ media and then streaking them onto 100 mM, 2 mM, or 0.4 mM K^+ plates. After verifying the growth phenotype of a portion of surviving colonies on 0.2 mM or 0.4 mM K^+ media, the total number of true positives was estimated to determine the percent rescue (the estimated total number of surviving colonies divided by the total number of colonies screened).

Electrophysiology

Wild-type and mutant *KAT1* with a C-terminal HA tag linked via a BglII site, subcloned into the pLin vector (Yi et al., 2001) at the HindIII-XhoI restriction sites, were transcribed using the AmpliCap T7 High Yield Message Maker Kit (Epicentre Technologies, Madison, WI) to generate cRNA. 5 ng or 30 ng of KAT wild-type or 30 ng of mutant cRNAs in 50 nL were injected into stage V-VI *Xenopus laevis* oocytes, which were recorded via two-electrode voltage clamp (GeneClamp 500B, Axon Instruments, Foster City, CA) 4–6 days after injection (filter frequency, 500 Hz; sampling frequency, 2 kHz; pipet resistance, 0.4–1.5 MΩ), using the following recording solutions. High-K^+ solution: 90 mM K(MES), 1 mM $Mg(MES)_2$, 1.8 mM $Ca(MES)_2$, 10 mM HEPES, pH to 7.4 with 10 N KOH; barium-blocking solution: 90 mM K(MES), 1 mM $Mg(MES)_2$, 1.8 mM $Ca(MES)_2$, 10 mM HEPES, 1 mM $Ba(MES)_2$, pH to 7.4 with 10 N KOH; barium- and TEA-blocking solution: 90 mM K(MES), 1 mM $Mg(MES)_2$, 1.8 mM $Ca(MES)_2$, 10 mM HEPES, 1 mM $Ba(MES)_2$, 10 mM TEA(MES), pH to 7.4 with 10 N KOH. Sorbitol was added to ensure the same osmolality for each solution. Exchange of solutions entailed perfusing 2 ml solutions into the oocyte chamber (300 μl volume). The pClamp software (Axon Instruments, Foster City, CA) was used for recording and analysis and Origin (Northampton, MA) or Microsoft Excel (Redmond, WA) for plotting graphs, traces, and data analysis. Statistical significance was determined using an unpaired two-tailed t test.

Western Blotting

Homogenate of five oocytes, taken 6 days after cRNA injection of a particular cRNA (3 days for wild-type) and homogenized by pipeting up and down in 50 μl lysis buffer (20 mM Tris pH 7.5, 150 mM NaCl, 0.5% Triton, 1× Complete Protease Inhibitor Cocktail tablet [Roche, Indianapolis, IN]), was cleared by centrifugation at 20,800 × g for 10 min at 4°C on a tabletop centrifuge. The supernatant (approximately 50 μL) was added to 12.5 μl 5× sample buffer (75 mM Tris pH 9.0, 12.5% glycerol, 10% SDS, 0.5 mM EDTA, 10 mM TCEP, bromophenol blue). After incubation at 75°C for 30 min, 15 μl of each sample was loaded onto a 10% SDS-PAGE gel with a 4% stacking gel. The gel was run for 1.5 hr at 100 V and blotted onto nitrocellulose overnight at 30 mV using the BioRad Ready-Gel mini gel system (Hercules, CA) in the following transfer buffer: 10 mM $NaHCO_3$, 3 mM Na_2CO_3, 0.025% SDS, 20% methanol. The Western blot was blocked with 5% milk/TBST (20 mM Tris pH 7.5, 150 mM NaCl, and 0.05% Tween) and probed with the 3F10 rat anti-HA antibody (Roche, Indianapolis, IN) for the primary antibody and a goat anti-rat F(ab′)2 HRP antibody (Jackson ImmunoResearch Laboratories, West Grove, PA) as the secondary antibody. Bands were visualized by chemiluminescence, exposed on film for 15 s to 5 min, and quantified using the AlphaImager 2200 system (Alpha Innotech Corporation, San Leandro, CA).

Wild-type and mutant KAT1 channels with a C-terminal HA tag expressed in yeast were grown to 0.7–0.9 O.D. in 100 mM K^+ SD -URA/-MET media and 2 O.D.s were harvested at 500 × g. The pellet was resuspended in 100 μl of 1× sample buffer and 0.2 g of acid-washed glass beads (425–600 μm). Samples were vortexed for 90 s, centrifuged at 14000 × g, and the supernatant sample retained. The samples were then denatured, separated, and blotted as described for the oocyte Western blot.

Modeling and Sequence Alignments

Modeller6v2 was used to construct a three-dimensional model of the KAT1 central pore (S5–S6) based upon the crystal structure of KvAP (Jiang et al., 2003a; Sali and Blundell, 1993). A truncated form of the KvAP central pore, consisting of K147-V240, was used as a template, and onto this was modeled Y193-S312 of KAT1. The

sequence alignment was an extension of an earlier alignment (Shealy et al., 2003), from the AKT subfamily to the KAT1 subfamily determined from our alignment. One hundred initial models were made. From these models, the one with the lowest objective energy function was used as a starting point for creating 100 additional models, which had 4-fold symmetry imposed upon each of the subunits and α-helical restraints placed upon the S5 and S6 segments. Again, the model with the lowest objective energy function was selected and is represented in Figure 2B.

Fluorescence Microscopy

KAT1 wild-type and mutants were C-terminally tagged with EGFP via an AgeI site and subcloned into the modified pYES2 vector (Minor et al., 1999; Yi et al., 2001) at the HindIII-XhoI restriction sites. Yeast expressing the KAT1-EGFP wt and mutants were grown to an O.D. of 0.5–1 in 100 mM K^+ SD-URA/-MET media. Cells were fixed with 2% formaldehyde for 15 min at room temperature, harvested at 1500 × g for 2 min, resuspended in 0.5 ml 100 mM potassium phosphate, pH 6.6, incubated for 10 min at room temperature, harvested at 1500 × g for 2 min, and resuspended in 25 μl of 100 mM potassium phosphate, pH 6.6. 5 μl of the cell suspension was mixed with 5 μl of mounting media (Biomeda Corporation, Foster City, CA) on a glass slide and overlaid with a cover slip. Cells were visualized using a Nikon Eclipse E800 Epifluorescence Compound Microscope (Melville, NY) with a 100× objective and 1 s exposure time. Pixel intensity was determined using ImageJ (Rasband, 1997-2005).

Supplemental Data

The Supplemental Data for this article can be found online at http://www.neuron.org/cgi/content/full/47/3/395/DC1/.

Acknowledgments

We would like to thank Dr. J.I. Schroeder for the KAT1 construct; Dr. S. Kurtz for providing the yeast strain; Dr. D. Minor for valuable experimental guidance; Dr. D. Bichet, Dr. B. Cohen, A. Fay, Dr. C. Gu, F. Haass, P. Haddick, Dr. B. Schroeder, T. Surti, Dr. B. Tu, and members of the Jan Lab for their support, helpful advice, and input at all stages of this project. H.C.L. is supported by an American Heart Association Pre-doctoral Fellowship, Western States Affiliate and was supported by an NIH Structural Biology Training Grant GM08284. M.G. is supported by a National Science Foundation Interdisciplinary Informatics Fellowship. Y.N.J. and L.Y.J. are HHMI investigators. This study is supported by an R01 grant from the NIMH. The authors declare no competing interests.

Received: November 9, 2004
Revised: March 9, 2005
Accepted: June 9, 2005
Published: August 3, 2005

References

Aggarwal, S.K., and MacKinnon, R. (1996). Contribution of the S4 segment to gating charge in the Shaker K+ channel. Neuron *16*, 1169–1177.

Ahern, C.A., and Horn, R. (2004). Specificity of charge-carrying residues in the voltage sensor of potassium channels. J. Gen. Physiol. *123*, 205–216.

Anderson, J.A., Huprikar, S.S., Kochian, L.V., Lucas, W.J., and Gaber, R.F. (1992). Functional expression of a probable Arabidopsis thaliana potassium channel in Saccharomyces cerevisiae. Proc. Natl. Acad. Sci. USA *89*, 3736–3740.

Ashcroft, F.M. (2000). Ion Channels and Diseases (London: Academic Press).

Bezanilla, F. (2000). The voltage sensor in voltage-dependent ion channels. Physiol. Rev. *80*, 555–592.

Bezanilla, F. (2002). Voltage sensor movements. J. Gen. Physiol. *120*, 465–473.

Broomand, A., Mannikko, R., Larsson, H.P., and Elinder, F. (2003). Molecular movement of the voltage sensor in a K channel. J. Gen. Physiol. *122*, 741–748.

Brownlee, C. (2002). Plant K+ transport: not just an uphill struggle. Curr. Biol. *12*, R402–R404.

Cao, Y., Crawford, N.M., and Schroeder, J.I. (1995). Amino terminus and the first four membrane-spanning segments of the Arabidopsis K+ channel KAT1 confer inward-rectification property of plant-animal chimeric channels. J. Biol. Chem. *270*, 17697–17701.

Cohen, B.E., Grabe, M., and Jan, L.Y. (2003). Answers and questions from the KvAP structures. Neuron *39*, 395–400.

Crunelli, V., and Leresche, N. (2002). Childhood absence epilepsy: genes, channels, neurons and networks. Nat. Rev. Neurosci. *3*, 371–382.

Cuello, L.G., Cortes, D.M., and Perozo, E. (2004). Molecular architecture of the KvAP voltage-dependent K+ channel in a lipid bilayer. Science *306*, 491–495.

Decher, N., Chen, J., and Sanguinetti, M.C. (2004). Voltage-dependent gating of hyperpolarization-activated, cyclic nucleotide-gated pacemaker channels: molecular coupling between the S4–S5 and C-linkers. J. Biol. Chem. *279*, 13859–13865.

Doyle, D.A. (2004). Structural changes during ion channel gating. Trends Neurosci. *27*, 298–302.

Eriksson, A.E., Baase, W.A., Zhang, X.J., Heinz, D.W., Blaber, M., Baldwin, E.P., and Matthews, B.W. (1992). Response of a protein structure to cavity-creating mutations and its relation to the hydrophobic effect. Science *255*, 178–183.

Gandhi, C.S., and Isacoff, E.Y. (2002). Molecular models of voltage sensing. J. Gen. Physiol. *120*, 455–463.

Gandhi, C.S., Clark, E., Loots, E., Pralle, A., and Isacoff, E.Y. (2003). The orientation and molecular movement of a k(+) channel voltage-sensing domain. Neuron *40*, 515–525.

Gaymard, F., Pilot, G., Lacombe, B., Bouchez, D., Bruneau, D., Boucherez, J., Michaux-Ferriere, N., Thibaud, J.B., and Sentenac, H. (1998). Identification and disruption of a plant shaker-like outward channel involved in K+ release into the xylem sap. Cell *94*, 647–655.

Gonzalez, C., Morera, F.J., Rosenmann, E., Alvarez, O., and Latorre, R. (2005). S3b amino acid residues do not shuttle across the bilayer in voltage-dependent Shaker K+ channels. Proc. Natl. Acad. Sci. USA *102*, 5020–5025.

Grabe, M., Lecar, H., Jan, Y.N., and Jan, L.Y. (2004). A quantitative assessment of models for voltage-dependent gating of ion channels. Proc. Natl. Acad. Sci. USA *102*, 5020–5025.

Gulbis, J.M., and Doyle, D.A. (2004). Potassium channel structures: do they conform? Curr. Opin. Struct. Biol. *14*, 440–446.

Hessa, T., White, S.H., and von Heijne, G. (2005). Membrane insertion of a potassium-channel voltage sensor. Science *307*, 1427.

Hille, B. (2001). Ion Channels of Excitable Membranes, Third Edition (Sunderland, MA: Sinauer).

Horn, R. (2002). Coupled movements in voltage-gated ion channels. J. Gen. Physiol. *120*, 449–453.

Hoshi, T. (1995). Regulation of voltage dependence of the KAT1 channel by intracellular factors. J. Gen. Physiol. *105*, 309–328.

Hosy, E., Vavasseur, A., Mouline, K., Dreyer, I., Gaymard, F., Poree, F., Boucherez, J., Lebaudy, A., Bouchez, D., Very, A.A., et al. (2003). The Arabidopsis outward K+ channel GORK is involved in regulation of stomatal movements and plant transpiration. Proc. Natl. Acad. Sci. USA *100*, 5549–5554.

Jiang, Y., Lee, A., Chen, J., Ruta, V., Cadene, M., Chait, B.T., and MacKinnon, R. (2003a). X-ray structure of a voltage-dependent K+ channel. Nature *423*, 33–41.

Jiang, Y., Ruta, V., Chen, J., Lee, A., and MacKinnon, R. (2003b). The principle of gating charge movement in a voltage-dependent K+ channel. Nature *423*, 42–48.

Jiang, Q.X., Wang, D.N., and MacKinnon, R. (2004). Electron microscopic analysis of KvAP voltage-dependent K+ channels in an open conformation. Nature *430*, 806–810.

Ko, C.H., and Gaber, R.F. (1991). TRK1 and TRK2 encode structur-

ally related K+ transporters in Saccharomyces cerevisiae. Mol. Cell. Biol. *11*, 4266–4273.

Kuo, A., Gulbis, J.M., Antcliff, J.F., Rahman, T., Lowe, E.D., Zimmer, J., Cuthbertson, J., Ashcroft, F.M., Ezaki, T., and Doyle, D.A. (2003). Crystal structure of the potassium channel KirBac1.1 in the closed state. Science *300*, 1922–1926.

Kuruma, A., Hirayama, Y., and Hartzell, H.C. (2000). A hyperpolarization- and acid-activated nonselective cation current in Xenopus oocytes. Am. J. Physiol. Cell Physiol. *279*, C1401–C1413.

Laine, M., Lin, M.C., Bannister, J.P., Silverman, W.R., Mock, A.F., Roux, B., and Papazian, D.M. (2003). Atomic proximity between S4 segment and pore domain in Shaker potassium channels. Neuron *39*, 467–481.

Latorre, R., Munoz, F., Gonzalez, C., and Cosmelli, D. (2003a). Structure and function of potassium channels in plants: some inferences about the molecular origin of inward rectification in KAT1 channels (Review). Mol. Membr. Biol. *20*, 19–25.

Latorre, R., Olcese, R., Basso, C., Gonzalez, C., Munoz, F., Cosmelli, D., and Alvarez, O. (2003b). Molecular coupling between voltage sensor and pore opening in the Arabidopsis inward rectifier K+ channel KAT1. J. Gen. Physiol. *122*, 459–469.

Lee, H.C., Wang, J.M., and Swartz, K.J. (2003). Interaction between extracellular Hanatoxin and the resting conformation of the voltage-sensor paddle in Kv channels. Neuron *40*, 527–536.

Li-Smerin, Y., Hackos, D.H., and Swartz, K.J. (2000). A localized interaction surface for voltage-sensing domains on the pore domain of a K+ channel. Neuron *25*, 411–423.

LiCata, V.J., and Ackers, G.K. (1995). Long-range, small magnitude nonadditivity of mutational effects in proteins. Biochemistry *34*, 3133–3139.

Lu, Z., Klem, A.M., and Ramu, Y. (2002). Coupling between voltage sensors and activation gate in voltage-gated K+ channels. J. Gen. Physiol. *120*, 663–676.

Ludwig, A., Zong, X., Stieber, J., Hullin, R., Hofmann, F., and Biel, M. (1999). Two pacemaker channels from human heart with profoundly different activation kinetics. EMBO J. *18*, 2323–2329.

Mannikko, R., Elinder, F., and Larsson, H.P. (2002). Voltage-sensing mechanism is conserved among ion channels gated by opposite voltages. Nature *419*, 837–841.

Marten, I., and Hoshi, T. (1998). The N-terminus of the K channel KAT1 controls its voltage-dependent gating by altering the membrane electric field. Biophys. J. *74*, 2953–2962.

Minor, D.L., Jr., Masseling, S.J., Jan, Y.N., and Jan, L.Y. (1999). Transmembrane structure of an inwardly rectifying potassium channel. Cell *96*, 879–891.

Mordoch, S.S., Granot, D., Lebendiker, M., and Schuldiner, S. (1999). Scanning cysteine accessibility of EmrE, an H+-coupled multidrug transporter from Escherichia coli, reveals a hydrophobic pathway for solutes. J. Biol. Chem. *274*, 19480–19486.

Mura, C.V., Cosmelli, D., Munoz, F., and Delgado, R. (2004). Orientation of Arabidopsis thaliana KAT1 channel in the plasma membrane. J. Membr. Biol. *201*, 157–165.

Neale, E.J., Elliott, D.J., Hunter, M., and Sivaprasadarao, A. (2003). Evidence for intersubunit interactions between S4 and S5 transmembrane segments of the Shaker potassium channel. J. Biol. Chem. *278*, 29079–29085.

Rasband, W.S. (1997–2005). ImageJ (computer program). U.S. National Institutes of Health. Bethesda, Maryland (http://rsb.info.nih.gov/ij/).

Rodriguez-Navarro, A. (2000). Potassium transport in fungi and plants. Biochim. Biophys. Acta *1469*, 1–30.

Ruta, V., Jiang, Y., Lee, A., Chen, J., and MacKinnon, R. (2003). Functional analysis of an archaebacterial voltage-dependent K+ channel. Nature *422*, 180–185.

Sali, A., and Blundell, T.L. (1993). Comparative protein modelling by satisfaction of spatial restraints. J. Mol. Biol. *234*, 779–815.

Sands, Z., Grottesi, A., and Sansom, M.S. (2005). Voltage-gated ion channels. Curr. Biol. *15*, R44–R47.

Sato, Y., Sakaguchi, M., Goshima, S., Nakamura, T., and Uozumi, N. (2002). Integration of Shaker-type K+ channel, KAT1, into the endoplasmic reticulum membrane: synergistic insertion of voltage-sensing segments, S3–S4, and independent insertion of pore-forming segments, S5-P-S6. Proc. Natl. Acad. Sci. USA *99*, 60–65.

Sato, Y., Sakaguchi, M., Goshima, S., Nakamura, T., and Uozumi, N. (2003). Molecular dissection of the contribution of negatively and positively charged residues in S2, S3, and S4 to the final membrane topology of the voltage sensor in the K+ channel, KAT1. J. Biol. Chem. *278*, 13227–13234.

Schachtman, D.P., Schroeder, J.I., Lucas, W.J., Anderson, J.A., and Gaber, R.F. (1992). Expression of an inward-rectifying potassium channel by the Arabidopsis KAT1 cDNA. Science *258*, 1654–1658.

Schreiber, G., and Fersht, A.R. (1995). Energetics of protein-protein interactions: analysis of the barnase-barstar interface by single mutations and double mutant cycles. J. Mol. Biol. *248*, 478–486.

Schroeder, J.I., Ward, J.M., and Gassmann, W. (1994). Perspectives on the physiology and structure of inward-rectifying K+ channels in higher plants: biophysical implications for K+ uptake. Annu. Rev. Biophys. Biomol. Struct. *23*, 441–471.

Seoh, S.A., Sigg, D., Papazian, D.M., and Bezanilla, F. (1996). Voltage-sensing residues in the S2 and S4 segments of the Shaker K+ channel. Neuron *16*, 1159–1167.

Serrano, R., and Rodriguez-Navarro, A. (2001). Ion homeostasis during salt stress in plants. Curr. Opin. Cell Biol. *13*, 399–404.

Sesti, F., Rajan, S., Gonzalez-Colaso, R., Nikolaeva, N., and Goldstein, S.A. (2003). Hyperpolarization moves S4 sensors inward to open MVP, a methanococcal voltage-gated potassium channel. Nat. Neurosci. *6*, 353–361.

Shealy, R.T., Murphy, A.D., Ramarathnam, R., Jakobsson, E., and Subramaniam, S. (2003). Sequence-function analysis of the K+-selective family of ion channels using a comprehensive alignment and the KcsA channel structure. Biophys. J. *84*, 2929–2942.

Shieh, C.C., Coghlan, M., Sullivan, J.P., and Gopalakrishnan, M. (2000). Potassium channels: molecular defects, diseases, and therapeutic opportunities. Pharmacol. Rev. *52*, 557–594.

Sigworth, F.J. (1994). Voltage gating of ion channels. Q. Rev. Biophys. *27*, 1–40.

Starace, D.M., and Bezanilla, F. (2004). A proton pore in a potassium channel voltage sensor reveals a focused electric field. Nature *427*, 548–553.

Swartz, K.J. (2004). Towards a structural view of gating in potassium channels. Nat. Rev. Neurosci. *5*, 905–916.

Tempel, B.L., Papazian, D.M., Schwarz, T.L., Jan, Y.N., and Jan, L.Y. (1987). Sequence of a probable potassium channel component encoded at Shaker locus of Drosophila. Science *237*, 770–775.

Thompson, J.D., Higgins, D.G., and Gibson, T.J. (1994). CLUSTAL W: improving the sensitivity of progressive multiple sequence alignment through sequence weighting, position-specific gap penalties and weight matrix choice. Nucleic Acids Res. *22*, 4673–4680.

Tiwari-Woodruff, S.K., Schulteis, C.T., Mock, A.F., and Papazian, D.M. (1997). Electrostatic interactions between transmembrane segments mediate folding of Shaker K+ channel subunits. Biophys. J. *72*, 1489–1500.

Tombola, F., Pathak, M.M., and Isacoff, E.Y. (2005). Voltage-sensing arginines in a potassium channel permeate and occlude cation-selective pores. Neuron *45*, 379–388.

Tristani-Firouzi, M., Chen, J., and Sanguinetti, M.C. (2002). Interactions between S4–S5 linker and S6 transmembrane domain modulate gating of HERG K+ channels. J. Biol. Chem. *277*, 18994–19000.

Uozumi, N., Nakamura, T., Schroeder, J.I., and Muto, S. (1998). Determination of transmembrane topology of an inward-rectifying potassium channel from Arabidopsis thaliana based on functional expression in Escherichia coli. Proc. Natl. Acad. Sci. USA *95*, 9773–9778.

Very, A.A., and Sentenac, H. (2003). Molecular mechanisms and regulation of K+ transport in higher plants. Annu. Rev. Plant Biol. *54*, 575–603.

Wells, J.A. (1990). Additivity of mutational effects in proteins. Biochemistry *29*, 8509–8517.

Yellen, G. (2002). The voltage-gated potassium channels and their relatives. Nature *419*, 35–42.

Yi, B.A., Lin, Y.F., Jan, Y.N., and Jan, L.Y. (2001). Yeast screen for constitutively active mutant G protein-activated potassium channels. Neuron *29*, 657–667.

Zei, P.C., and Aldrich, R.W. (1998). Voltage-dependent gating of single wild-type and S4 mutant KAT1 inward rectifier potassium channels. J. Gen. Physiol. *112*, 679–713.